Model-informed COVID-19 vaccine prioritization strategies by age and serostatus

Kate M. Bubar,[1,2*] Kyle Reinholt,[3] Stephen M. Kissler,[4] Marc Lipsitch[4,5], Sarah Cobey[6], Yonatan H. Grad[4], Daniel B. Larremore[3,7*]

[1]Department of Applied Mathematics, University of Colorado Boulder, Boulder, CO, 80303, USA
[2]IQ Biology Program, University of Colorado Boulder, Boulder, CO, 80309, USA
[3]Department of Computer Science, University of Colorado Boulder, Boulder, CO, 80309, USA
[4]Department of Immunology and Infectious Diseases, Harvard T.H. Chan School of Public Health, Boston, MA, 02115, USA
[5]Center for Communicable Disease Dynamics, Harvard T.H. Chan School of Public Health, Boston, MA, 02115, USA
[6]Department of Ecology and Evolution, University of Chicago, Chicago, IL, 60637, USA
[7]BioFrontiers Institute, University of Colorado Boulder, Boulder, CO, 80303, USA

*To whom correspondence should be addressed;
E-mail: kate.bubar@colorado.edu and daniel.larremore@colorado.edu

Limited initial supply of SARS-CoV-2 vaccine raises the question of how to prioritize available doses. Here, we used a mathematical model to compare five age-stratified prioritization strategies. A highly effective transmission-blocking vaccine prioritized to adults ages 20-49 years minimized cumulative incidence, but mortality and years of life lost were minimized in most scenarios when the vaccine was prioritized to adults over 60 years old. Use of individual-level serological tests to redirect doses to seronegative individuals improved the marginal impact of each dose while partially addressing existing inequities in COVID-19 impact. While maximum impact prioritization strategies were broadly consistent across countries, transmission rates, vaccination rollout speeds, and estimates of naturally acquired immunity, this framework can be used to compare impacts of prioritization strategies across contexts.

SARS-CoV-2 has caused a public health and economic crisis worldwide. As of November 2020, there have been over 62 million cases and 1.4 million deaths reported (*1*). To combat this crisis, a variety of non-pharmaceutical interventions have been implemented, including shelter-in-place orders, limited travel, and remote schooling. While these efforts are essential to slowing transmission in the short term, long-term solutions—such as vaccines that protect from SARS-CoV-2 infection—are urgently needed.

As the benefits of an effective vaccine for individuals and their communities may result in widespread demand, it is critical that decision-making on vaccine distribution is well motivated, particularly in the initial phases when vaccine availability may be limited (*2*).

Here, we employ a model-informed approach to quantify the impact of COVID-19 vaccine prioritization strategies on cumulative incidence and mortality. Our approach explicitly addresses variation in three areas that can influence the outcome of vaccine distribution decisions. First, we consider variation in the performance of the vaccine, including its overall efficacy, a hypothetical decrease in efficacy by age, and the vaccine's ability to block transmission. Second, we consider variation in both susceptibility to infection and the infection fatality rate by age. Third, we consider variation in the population and policy, including the age distribution, age-stratified contact rates, and initial fraction of seropositive individuals by age, and the speed and timing of the vaccine's rollout relative to transmission. While the earliest doses of vaccines will be given to front-line health care workers under plans such as those from the COVAX initiative and the US NASEM recommendations (*3*), our work is focused on informing the prioritization of the doses that follow.

There are two main approaches to vaccine prioritization: (1) directly vaccinate those at highest risk and (2) protect them indirectly by vaccinating those who do the most transmitting. Model-based investigations of the tradeoffs between these strategies for influenza vaccination have led to recommendations that children be vaccinated due to their critical role in transmission (*4, 5*), and have shown that direct protection is superior when reproduction numbers are high but indirect protection is superior when transmissibility is low (*6*). Similar modeling for COVID-19 vaccination has found that the optimal balance between direct and indirect protection depends on both vaccine efficacy and supply, recommending direct vaccination of older adults for low-efficacy vaccines and for high-efficacy but supply-limited vaccines (*7*). Rather than comparing prioritization strategies, others have compared hypothetical vaccines, showing that even those with lower efficacy for direct protection may be more valuable if they also provide better indirect protection by blocking transmission (*8*). Prioritization of transmission-blocking

vaccines can also be dynamically updated based on the current state of the epidemic, shifting prioritization to avoid decreasing marginal returns (*9*). These efforts to prioritize and optimize doses complement other work showing that, under a variety of scenarios of vaccine efficacy and durability of immunity, the economic and health benefits of COVID-19 vaccines will be large in the short and medium terms (*10*). The problem of vaccine prioritization also parallels the more general problem of optimal resource allocation to reduce transmission, e.g. with masks (*11*).

Evaluation of vaccine prioritization strategies

We evaluated the impact of vaccine prioritization strategies using an age-stratified SEIR model, because age has been shown to be an important correlate of susceptibility (*12–14*), seroprevalence (*12, 15*), severity (*16–18*), and mortality (*19, 20*). This model includes an age-dependent contact matrix, susceptibility to infection, and infection fatality rate (IFR), allowing us to estimate cumulative incidence of SARS-CoV-2 infections, mortality due to infection, and years of life lost (YLL; see Methods) via forward simulations. Cumulative incidence, mortality, and YLL were then used as outcomes by which to compare vaccine prioritization strategies.

We first examined the impact of five vaccine prioritization strategies for a hypothetical infection- and transmission-blocking vaccine of varying efficacy. The strategies prioritized vaccines to (1) children and teenagers, (2) adults between ages 20 and 49 years, (3) adults 20 years or older, (4) adults 60 years or older, and (5) all individuals (Figure 1A). In all strategies, once the prioritized population was fully vaccinated, vaccines were allocated irrespective of age.

We measured reductions in cumulative incidence, mortality, and YLL achieved by each strategy, varying the vaccine supply between 1% and 50% of the total population, under three scenarios. In Scenario 1, vaccines were administered to 1% of the population per day until supply was exhausted, with $R_0 = 1.3$, representing mitigated spread during vaccine rollout. In Scenario 2, vaccines were administered to 1% of the population per day until supply was exhausted, but with $R_0 = 2.6$, representing

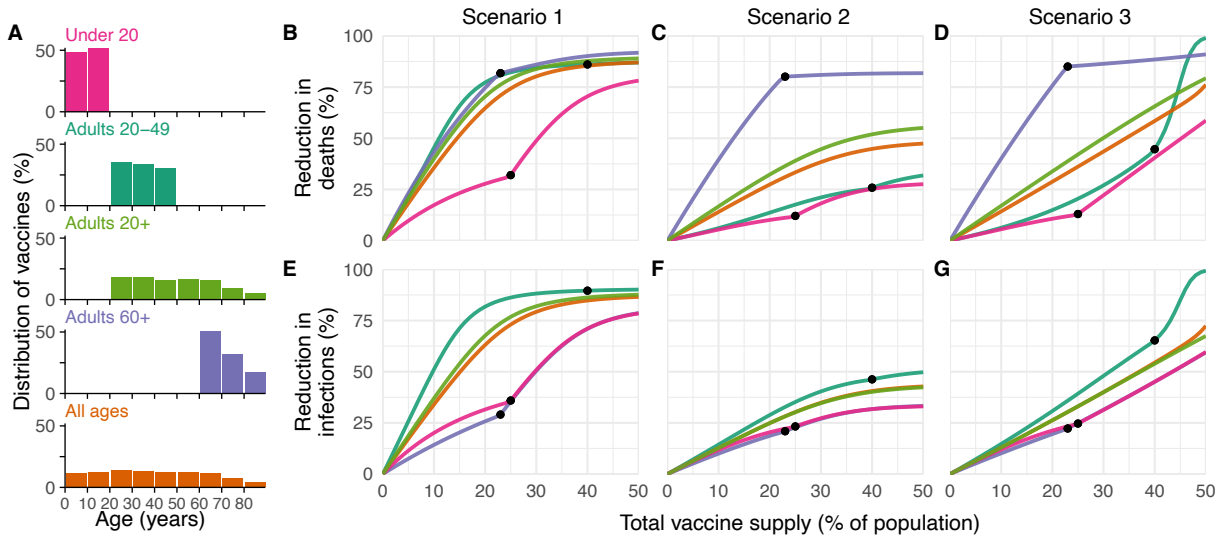

Figure 1: **Impacts of vaccine prioritization strategies on mortality and infections.** (A) Distribution of vaccines for five prioritization strategies: under 20, adults 20-49, adults 20+, adults 60+ and all ages. (B, C, D) Percent reductions in deaths and (E, F, G) infections in comparison to an unmitigated outbreak, covering Scenario 1 (1% rollout/day, $R_0 = 1.3$; B, E), Scenario 2 (1% rollout/day, $R_0 = 2.6$; C, F), and Scenario 3 (anticipatory rollout, $R_0 = 2.6$; D, G). Black dots indicate breakpoints at which prioritized demographic groups have been fully vaccinated, after which vaccines are distributed without prioritization. These simulations assume contact patterns and demographics of the United States (*21, 22*) and an all-or-nothing, transmission-blocking vaccine with $ve = 90\%$.

unmitigated spread during vaccine rollout. In Scenario 3, vaccines were administered before transmission began, referred to as anticipatory rollout, with $R_0 = 2.6$. We considered two ways in which vaccine efficacy (ve) could be below 100%: an all-or-nothing vaccine, where the vaccine provides perfect protection to a fraction ve of individuals who receive it, or as a leaky vaccine, where all vaccinated individuals have reduced probability ve of infection after vaccination (see Methods).

Of the five strategies, direct vaccination of adults over 60 years (60+) nearly always reduced mortality and YLL more than the alternative strategies when transmission was high ($R_0 = 2.6$; Scenarios 2 and 3; 90% efficacy, Fig. 1; 30%-100% efficacy, Fig. S2). Exceptions occurred only in anticipatory vaccination when vaccine efficacy was 80% or higher and supply was sufficient to cover over 45% of the population (Fig. S2). For lower transmission ($R_0 = 1.3$; Scenario 1), direct vaccination of adults 60+ reduced mortality more than the alternative strategies when vaccine supply was low ($< 8\%$ coverage)

or when both vaccine supply and efficacy were high ($> 35\%$ supply, $> 80\%$ efficacy) with vaccination of adults 20-49 providing slightly better reductions in mortality otherwise (Figs. 1 and S2). Prioritizing adults 20-49 minimized cumulative incidence in all three scenarios for all vaccine efficacies (Figs. 1 and S2). Findings for Scenario 2 were unaffected by vaccination rollout speed (0.25% to 2% per day), but faster rollout speeds increased the range of vaccine supply levels at which vaccination of adults 20-49 provided better mortality reduction in Scenario 1 (Fig. S3). Findings for mortality and YLL were only slightly changed by modeling vaccine efficacy as all-or-nothing (Fig. S2) or leaky (Fig. S4). However, to minimize incidence, optimal prioritization shifted to those under 20 y for low-efficacy leaky vaccines in Scenarios 1 and 2 (Fig. S4).

Impact of transmission rates, age demographics, and contact structure

To evaluate the impact of transmission rates on the strategy that most reduced mortality, we varied the basic reproductive number R_0 from 1.3 to 2.6 for a hypothetical infection- and transmission-blocking vaccine with $ve = 90\%$. We found that prioritizing adults 60+ remained the best way to reduce mortality and YLL for all vaccine supplies, unless transmission rates were low when the vaccine was rolled out during ongoing transmission ($R_0 \leq 1.5$); see Figs. 2A and S5). However, vaccinating prior to transmission revealed combinations of transmission rates and vaccine supplies for which vaccinating adults 20-49 or all adults 20+ were more effective (see Figs. 2B and S5). Prioritizing adults 20-49 minimized infections for all values of R_0 investigated (Fig. S5).

To determine whether our findings were robust across countries, we analyzed the ranking of prioritization strategies for populations with the age distributions and modeled contact structures of the United States, Belgium, Brazil, China, India, Poland, South Africa, and Spain. Across these countries, direct vaccination of adults 60+ minimized mortality for most levels of vaccine supply when transmission was high ($R_0 = 2.6$, Scenarios 2 and 3; Fig. 2C and D), but in only some cases when transmission was low ($R_0 = 1.3$, Scenario 1; Fig. 2E). Across countries, vaccination of adults 20-49 nearly always minimized

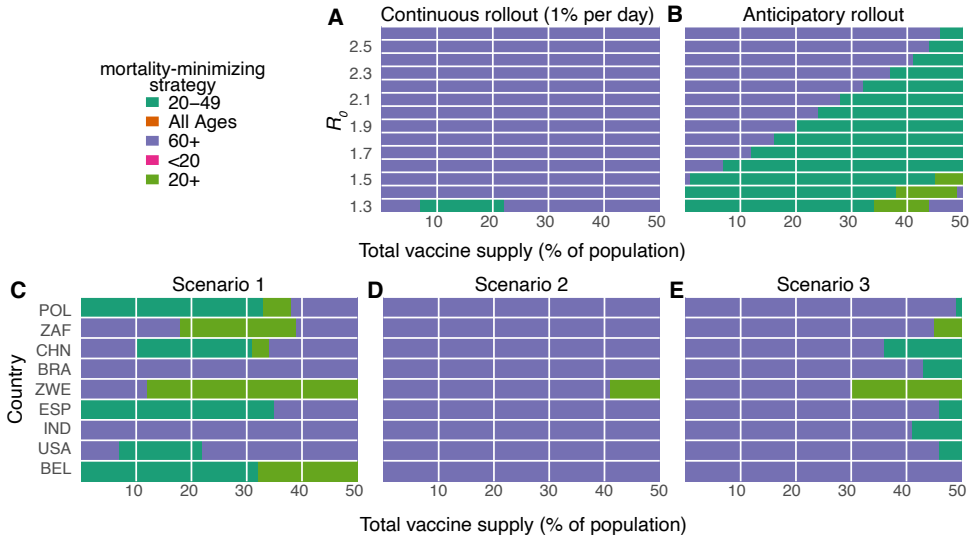

Figure 2: **Mortality-minimizing vaccine prioritization strategies across reproductive numbers R_0 and countries.** Heatmaps show the prioritization strategies resulting in maximum reduction of mortality for varying values of the basic reproductive number R_0 (A, B) and across nine countries (C, D, E), for vaccine supplies between 1% and 50% of the total population. (A, B) Shown: contact patterns and demographics of the United States (*21, 22*); all-or-nothing and transmission blocking vaccine; $ve = 90\%$ (C, D, E) Scenario 1: 1% rollout/day, $R_0 = 1.3$; Scenario 2: 1% rollout/day, $R_0 = 2.6$; Scenario 3: anticipatory rollout, $R_0 = 2.6$. Shown: all-or-nothing and transmission blocking vaccine, $ve = 90\%$. POL, Poland; ZAF, South Africa; CHN, China; BRA, Brazil; ZWE, Zimbabwe; ESP, Spain; IND, India; USA, United States of America; BEL, Belgium.

infections, and vaccination of adults 60+ nearly always minimized YLL for Scenarios 2 and 3, but no clear ranking of strategies emerged consistently to minimize YLL in Scenario 1 (Fig. S6).

Vaccines with imperfect transmission blocking effects

We also considered whether the rankings of prioritization strategies to minimize mortality would change if a vaccine were to block COVID-19 symptoms and mortality with 90% efficacy but with variable impact on SARS-CoV-2 infection and transmission. We found that direct vaccination of adults 60+ minimized mortality for all three Scenarios and for all vaccine supplies when up to 70% of transmission was blocked, and up to complete transmission blocking for most vaccine supply levels (Supplementary Text S1 and Supplementary Fig. S7).

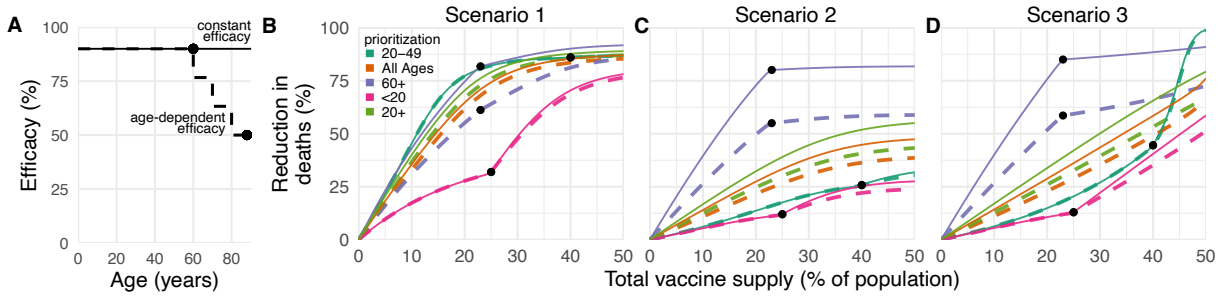

Figure 3: **Effects of age-dependent vaccine efficacy on the impacts of prioritization strategies.** (A) Diagram of hypothetical age-dependent vaccine efficacy shows decrease from 90% baseline efficacy to 50% efficacy among individuals 80+ beginning at age 60 (dashed line). (B, C, D) Percent reduction in deaths in comparison to an unmitigated outbreak for transmission-blocking all-or-nothing vaccines with either constant 90% efficacy for all age groups (solid lines) or age-dependent efficacy shown in panel A (dashed lines), covering Scenario 1 (1% rollout/day, $R_0 = 1.3$; B), Scenario 2 (1% rollout/day, $R_0 = 2.6$; C), and Scenario 3 (anticipatory rollout, $R_0 = 2.6$; D). Black dots indicate breakpoints at which prioritized demographic groups have been fully vaccinated, after which vaccines are distributed without prioritization. Shown: contact patterns and demographics of the United States (*21, 22*); all-or nothing and transmission blocking vaccine.

Variation in vaccine efficacy by age

COVID-19 vaccines may not be equally effective across age groups in preventing infection or transmission, a phenomenon known to affect influenza vaccines (*23–26*). To understand the impact of age-dependent COVID-19 vaccine efficacy, we incorporated a hypothetical linear decrease from a baseline efficacy of 90% for those under 60 y to 50% in those 80 y and older (Figure 3). As expected, this diminished the benefits of any prioritization strategy that included older adults. For instance, strategies prioritizing adults 20-49 were unaffected by decreased efficacy among adults 60+, while strategies prioritizing adults 60+ were markedly diminished (Fig 3). Despite these effects, prioritization of adults 60+ remained superior to the alternative strategies to minimize mortality in Scenarios 2 and 3.

To test whether more substantial age-dependent vaccine effects would change which strategy minimized mortality in Scenarios 2 and 3, we varied the onset age of age-dependent decreases in efficacy, the extent to which it decreased, and the baseline efficacy from which it decreased. We found that as long as vaccine efficacy among adults 80+ was at least 25%, prioritizing adults 60+ remained superior

in the overwhelming majority of parameter combinations and across vaccine supply levels. This finding was robust to varying population contact structure and demographics and whether the vaccine was modeled as leaky vs all-or-nothing (Fig. S8). Only when vaccine supplies neared 50% of the population, or when efficacy among adults 80+ dropped below 25%, did the best available strategy switch from direct vaccination of adults 60+ to an alternative.

Incorporation of population seroprevalence and individual serological testing

If naturally acquired antibodies correlate with protection from reinfection, seroprevalence will affect vaccine prioritization in two ways. First, depending on the magnitude and age distribution of seroprevalence at the time of vaccine distribution, the ranking of strategies could change. Second, distributing vaccines to seropositive individuals would reduce the marginal benefit of vaccination per dose.

To investigate the impact of vaccinating in mid-epidemic while potentially employing serology to target the vaccine to seronegative individuals, we included age-stratified seroprevalence estimates in our model by moving the data-specified proportion of seropositive individuals from susceptible to recovered status. We then simulated two approaches to vaccine distribution. First, vaccines were distributed according to the five prioritization strategies introduced above, regardless of any individual's serostatus. Second, vaccines were distributed with a serological test, such that individuals with a positive serological test would not be vaccinated, allowing their dose to be given to someone else.

We included age-stratified seroprevalence estimates from New York City [August 2020; overall seroprevalence 26.9% (*27*)], and demographics and age-contact structure the United States in evaluations of the previous five prioritization strategies. For this analysis, we focused on Scenario 2 (1% rollout per day, $R_0 = 2.6$ in the absence of seropositives), and found that the ranking of strategies to minimize incidence, mortality, and YLL remained unchanged: prioritizing adults 60+ most reduced mortality and prioritizing adults 20-49 most reduced incidence, regardless of whether vaccination was limited to seronegative individuals (Fig. 4). These rankings were unchanged when we used lower or higher age-stratified sero-

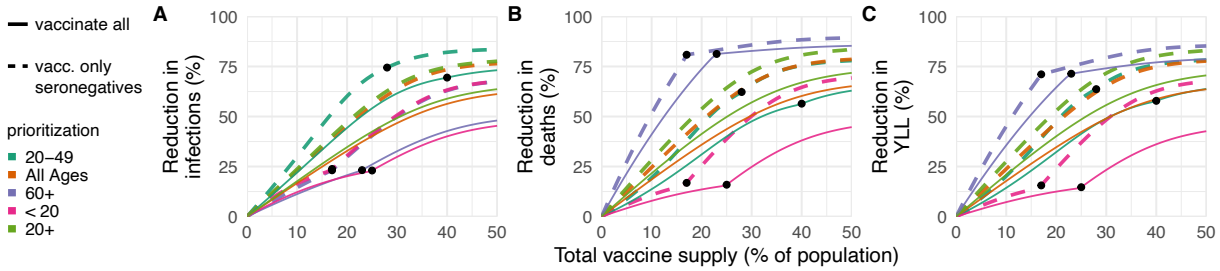

Figure 4: **Effects of existing seropositivity on the impacts of of prioritization strategies.** Percent reductions in (A) infections, (B) deaths, and (C) years of life lost (YLL) for prioritization strategies when existing age-stratified seroprevalence is incorporated (August 2020 estimates for New York City; mean seroprevalence 26.9% (*27*)). Plots show reductions for Scenario 2 (1% rollout/day, $R_0 = 2.6$, realized $R = 1.91$) when vaccines are given to all individuals (solid lines) or to only seronegatives (dashed lines), inclusive of imperfect serotest sensitivity and specificity. Shown: U.S. contact patterns and demographics (*21, 22*); all-or-nothing and transmission-blocking vaccine with $ve = 90\%$. See Figs. S9 and S10 for lower and higher seroprevalence examples, respectively.

prevalence estimates to test the consistency of results (Connecticut, July 2020, overall seroprevalence 3.4% (*28*) and synthetic, overall seroprevalence 39.5%; Figs. S9 and S10). Preferentially vaccinating seronegative individuals yielded large additional reductions in cumulative incidence and mortality in locations with higher seroprevalence (Figs. 4 and S10) and modest reductions in locations with low seroprevalence (Fig. S9). These results remained unchanged when statistical uncertainty, due to sample size and imperfect test sensitivity and specificity, were incorporated into the model (*29*).

Discussion

This study demonstrated the use of an age-stratified modeling approach to evaluate and compare vaccine prioritization strategies for SARS-CoV-2. After accounting for country-specific age structure, age-contact structure, infection fatality rates, and seroprevalence, as well as the age-varying efficacy of a hypothetical vaccine, we found that across countries those 60y and older should be prioritized to minimize deaths, assuming a return to pre-pandemic behavior during or after vaccine rollout. This recommendation is robust because of the dramatic differences in IFR by age. Our model identified two general regimes in which prioritizing all adults or adults aged 20-49 would provide greater mortality benefits than priori-

tizing older adults. One regime was restricted to the simultaneous conditions of transmission-mitigating behavior ($R_0 = 1.3$), vaccine efficacy 80% or below, and 90% or higher transmission blocking. Another regime was characterized by vaccines with very low efficacy in older adults, very high efficacy in younger adults, and declines in efficacy starting at 49 or 59, for a leaky vaccine, and even more restrictive conditions for an all-or-nothing vaccine. The advantage of prioritizing all adults or adults 20-49 vs. adults 60+ was small under these conditions. Thus, we conclude that for mortality reduction, prioritization of older adults is a robust strategy that will be optimal or close to optimal to minimize mortality for virtually all plausible vaccine characteristics.

In contrast, the ranking of infection-minimizing strategies depended on whether we considered an all-or-nothing vaccine or a leaky vaccine. Modeling all-or-nothing vaccines led to consistent recommendations to prioritize adults 20-49 across efficacy values and countries. However, for leaky vaccines, prioritization shifted toward children and teenagers for vaccine efficacy of 50%, in line with prior work (*7*). We also found that the transition point between top-ranked strategies varied by country demographics and contact patterns when considering a leaky vaccine. Because a vaccine is likely to have properties of both leaky and all-or-nothing models, empirical data on vaccine performance could help resolve this difference in model recommendations, although data are difficult to obtain in practice [see, e.g. (*30, 31*)].

It is not yet clear whether the first-generation of COVID-19 vaccines will be approved everywhere for the elderly or those under 18y (*32–34*). While our conclusions assumed that the vaccine would be approved for all age groups, the evaluation approaches introduced here can be tailored to evaluate a subset of approaches restricted to those within the age groups for which a vaccine is licensed, using open-source tools such as those that accompany this manuscript. Furthermore, while we considered three possible goals of vaccination— minimizing cumulative incidence, mortality, or YLL— our framework can be adapted to consider goals such as minimizing hospitalizations, ICU occupancy (*7*) or economic costs (*10*).

We demonstrated that there is value in pairing individual-level serological tests with vaccination, even

when accounting for the uncertainties in seroprevalence estimates (*29*). The marginal gain in effective vaccine supply, relative to no serological testing, must be weighed against the challenges of serological testing prior to vaccination. Serostatus itself is an imperfect indicator of protection, and the relationship of prior infection, serostatus, and protection may change over time (*10, 35*). Delays in serological tests results would impair vaccine distribution.

The best performing strategies depend on assumptions about the extent of a population's interactions. We used pre-pandemic contact matrices (*21*), reflecting the goal of a return to pre-pandemic routines once a vaccine is available, but more recent estimates of age-stratified contact rates could be valuable in modeling mid-pandemic scenarios (*36, 37*). The scenarios modeled here did not incorporate explicit non-pharmaceutical interventions, which might persist if vaccination coverage is incomplete, but are implicitly represented in Scenario 1 ($R_0 = 1.3$).

Our study relies on estimates of other epidemiological parameters. In local contexts, these include age-structured seroprevalence and IFR, which vary by population (*19, 20, 38*). Globally, key parameters include the degree to which antibodies protect against reinfection or severity of disease and relative infectiousness by age. From vaccine trials, we also need evidence of efficacy in groups vulnerable to severe outcomes, including the elderly. Additionally, it will be critical to measure whether a vaccine that protects against symptomatic disease also blocks infection and transmission of SARS-CoV-2 (*39*).

The role of children during this pandemic has been unclear. Under our assumptions about susceptibility by age, children are not the major drivers of transmission in communities, consistent with emerging evidence (*12*). Thus, our results differ from the optimal distribution for influenza vaccines, which prioritize school-age children and adults age 30-39 (*5*). However, the relative susceptibility and infectiousness of SARS-CoV-2 by age remain uncertain. While it is unlikely that susceptibility to infection conditional on exposure is constant across age groups (*12*), we ran our model to test the sensitivity of this parameter. Under the scenario of constant susceptibility by age, vaccinating those under 20 has a greater impact on reducing cumulative cases than before, but the overall ranking of strategies remains the same

(Supplementary Figures S11, S12).

Our study is subject to a number of limitations. First, our evaluation strategy focuses on a single country at a time [rather than on between-population allocation (*40*)], and considers variation in disease severity only by age. However, other factors correlate with disease outcomes, such as treatment and healthcare access and comorbidities, which may correlate with factors like rural vs urban location, socioeconomic status, sex (*41, 42*), and race and ethnicity (*43*), that are not accounted for in this study. Inclusion of these factors in a model would be possible, but only with statistically sound measurements of both their stratified infection risk, contact rates, and disease outcomes. Even in the case of age stratification, contact surveys have typically not surveyed those 80 years and older, yet it is this population that suffers dramatically more severe COVID-19 disease and higher infection fatality rates. We extrapolated contact matrices to those older than 80, but direct measurements would be superior. Last, our study focused on guiding strategy rather than providing more detailed forecasting or estimates (*10*). As such, we have not made detailed parameter fits to time series of cases or deaths, but rather have used epidemiologic models to identify robust strategies across a range of transmission scenarios.

Our study also considers variation in disease risk only by age, via age-structured contact matrices and age-specific susceptibility, while many discussions around COVID-19 vaccine distribution have thus far focused on prioritizing healthcare or essential workers (*44, 45*). Contact rates, and thus infection potential, vary greatly not only by occupation and age but also by living arrangement (e.g., congregate settings, dormitories), neighborhood and mobility (*46–49*), and whether the population has a coordinated and fundamentally effective policy to control the virus. With a better understanding of population structure during the pandemic, and risk factors of COVID-19, these limitations could be addressed. Meanwhile, the robust findings in favor of prioritizing those age groups with the highest IFR to minimize mortality could potentially be extended to prioritize those with comorbidities that predispose them to a high IFR, since the strategy of prioritizing the older age groups depends on direct rather than indirect protection.

Vaccine prioritization is not solely a question of science but a question of ethics as well. Hallmarks

of the COVID-19 pandemic, as with other global diseases, are inequalities and disparities. While these modeling efforts focus on age and minimizing incidence and death within a simply structured population, other considerations are crucial, from equity in allocation between countries to disparities in access to healthcare, including vaccination, that vary by neighborhood. Thus, the model's simplistic representation of vulnerability (age) should be augmented by better information on the correlates of infection risk and severity. Fair vaccine prioritization should avoid further harming disadvantaged populations. We suggest that, after distribution, pairing serological testing with vaccination in the hardest hit populations is one possible equitable way to extend the benefits of vaccination in settings where vaccination might otherwise not be deemed cost-effective.

References

1. COVID-19 dashboard by the center for systems science and engineering at johns hopkins university. Online, 2020 (accessed November 30, 2020). https://coronavirus.jhu.edu/map.html.

2. Roxanne Khamsi. If a coronavirus vaccines arrives, can the world make enough? *Nature*, 580:578–580, April 2020.

3. Framework for equitable allocation of COVID-19 vaccine. Online, 2020 (accessed December 6, 2020). https://www.nap.edu/catalog/25917/framework-for-equitable-allocation-of-covid-19-vaccine.

4. Derek Weycker, John Edelsberg, M. Elizabeth Halloran, Ira M. Longini, Azhar Nizam, Vincent Ciuryla, and Gerry Oster. Population-wide benefits of routine vaccination of children against influenza. *Vaccine*, 23(10):1284 – 1293, 2005.

5. Jan Medlock and Alison P. Galvani. Optimizing influenza vaccine distribution. *Science*, 325, 2009.

6. Shweta Bansal, Babak Pourbohloul, and Lauren Ancel Meyers. A comparative analysis of influenza vaccination programs. *PLoS Medicine*, 3(10):e387, 2006.

7. Laura Matrajt, Julie Eaton, Tiffany Leung, and Elizabeth R Brown. Vaccine optimization for COVID-19, who to vaccinate first? *medRxiv*, 2020. https://www.medrxiv.org/content/early/2020/08/16/2020.08.14.20175257.

8. Molly E. Gallagher, Andrew J. Sieben, Kristin N. Nelson, Alicia N. M. Kraay, Ben Lopman, Andreas Handel, and Katia Koelle. Considering indirect benefits is critical when evaluating SARS-CoV-2 vaccine candidates. *medRxiv*, 2020. https://www.medrxiv.org/content/early/2020/08/11/2020.08.07.20170456.

9. Jack Hoyt Buckner, Gerardo Chowell, and Michael R Springborn. Dynamic prioritization of covid-19 vaccines when social distancing is limited for essential workers. *medRxiv*, 2020. https://www.medrxiv.org/content/10.1101/2020.09.22.20199174v4.

10. Frank Sandmann, Nicholas Davies, Anna Vassall, W John Edmunds, Mark Jit, et al. The potential health and economic value of sars-cov-2 vaccination alongside physical distancing in the uk: transmission model-based future scenario analysis and economic evaluation. *medRxiv*, 2020. https://www.medrxiv.org/content/10.1101/2020.09.24.20200857v1.

11. Colin J. Worby and Hsiao-Han Chang. Face mask use in the general population and optimal resource allocation during the COVID-19 pandemic. *Nature Communications*, 11(4049), 2020.

12. Edward Goldstein, Marc Lipsitch, and Muge Cevik. On the effect of age on the transmission of SARS-CoV-2 in households, schools and the community. *The Journal of Infectious Diseases*, October 2020.

13. Nicholas Davies, Petra Klepac, Yang Liu, Kiesha Prem, Mark Jit, and Rosalind M Eggo. Age-dependent effects in the transmission and control of COVID-19 epidemics. *Nature Medicine*, 26(1205-1211), 2020.

14. Juanjuan Zhang, Maria Litvinova, Yuxia Liang, Yan Wang, Wei Wang, Shanlu Zhao, Qianhui Wu, Stefano Merler, Cécile Viboud, Alessandro Vespignani, Marco Ajelli, and Hongjie Yu. Changes in contact patterns shape the dynamics of the COVID-19 outbreak in China. *Science*, 368(6498):1481–1486, 2020.

15. Sereina Herzog, Jessie De Bie, Steven Abrams, Ine Wouters, Esra Ekinci, Lisbeth Patteet, Astrid Coppens, Sandy De Spiegeleer, Philippe Beutels, Pierre Van Damme, Niel Hens, and Heidi Theeten. Seroprevalence of igg antibodies against sars coronavirus 2 in belgium: a prospective cross-

sectional nationwide study of residual samples. *medRxiv*, 2020. https://www.medrxiv.org/content/early/2020/07/30/2020.06.08.20125179.

16. Amber L. Mueller, Maeve S. McNamara, and David A. Sinclair. Why does COVID-19 disproportionately affect older people? *Aging*, 12(10):9959–9981, 2020.

17. Yang Liu, Bei Mao, Shuo Liang, Jia-Wei Yang, Hai-Wen Lu, Yan-Hua Chai, Lan Wang, Li Zhang, Qiu-Hong Li, Lan Zhao, Yan He, Xiao-Long Gu, Xiao-Bin Ji, Li Li, Zhi-Jun Jie, Qiang Li, Xiang-Yang Li, Hong-Zhou Lu, Wen-Hong Zhang, Yuan-Lin Song, Jie-Ming Qu, and Jin-Fu Xu. Association between age and clinical characteristics and outcomes of COVID-19. *European Respiratory Journal*, 55(5):2001112, 2020.

18. Jaana Westmeier, Krystallenia Paniskaki, Zehra Karaköse, Tanja Werner, Kathrin Sutter, Sebastian Dolff, Marvin Overbeck, Andreas Limmer, Jia Liu, Xin Zheng, et al. Impaired cytotoxic cd8+ t cell response in elderly covid-19 patients. *MBio*, 11(5), 2020.

19. Andrew T Levin, Gideon Meyerowitz-Katz, Nana Owusu-Boaitey, Kensington B. Cochran, and Seamus P. Walsh. Assessing the age specificity of infection fatality rates for COVID-19: Systematic review, meta-analysis, and public policy implications. *medRxiv*, 2020.

20. Henrik Salje, Cécile Tran Kiem, Noémie Lefrancq, Noémie Courtejoie, Paolo Bosetti, Juliette Paireau, Alessio Andronico, Nathanaël Hozé, Jehanne Richet, Claire-Lise Dubost, Yann Le Strat, Justin Lessler, Daniel Levy-Bruhl, Arnaud Fontanet, Lulla Opatowski, Pierre-Yves Boelle, and Simon Cauchemez. Estimating the burden of SARS-CoV-2 in France. *Science*, 369(6500):208–211, 2020.

21. Kiesha Prem, Kevin van Zandvoort, Petra Klepac, Rosalind M Eggo, Nicholas G Davies, Alex R Cook, and Mark Jit. Projecting contact matrices in 177 geographical regions: an update and com-

parison with empirical data for the COVID-19 era. *medRxiv*, 2020. https://www.medrxiv.org/content/10.1101/2020.07.22.20159772v2.

22. United Nations Department of Economic and Social Affairs Population Division. World population prospects. Online, 2019 (accessed August 30, 2020). https://population.un.org/wpp/.

23. Peter A. Gross, Alicia W. Hermogenes, Henry S. Sacks, and Joseph Lau. The efficacy of influenza vaccine in elderly persons. *Annals of Internal Medicine*, 123(7):518–527, 1995. PMID: 7661497.

24. Jason K. H. Lee, Gary K. L. Lam, Thomas Shin, Jiyeon Kim, Anish Krishnan, David P. Greenberg, and Ayman Chit. Efficacy and effectiveness of high-dose versus standard-dose influenza vaccination for older adults: a systematic review and meta-analysis. *Expert Review of Vaccines*, 17(5):435–443, 2018. PMID: 29715054.

25. Th. M. E. Govaert, C. T. M. C. N. Thijs, N. Masurel, M. J. W. Sprenger, G. J. Dinant, and J. A. Knottnerus. The Efficacy of Influenza Vaccination in Elderly Individuals: A Randomized Double-blind Placebo-Controlled Trial. *JAMA*, 272(21):1661–1665, December 1994.

26. Joseph A Lewnard and Sarah Cobey. Immune history and influenza vaccine effectiveness. *Vaccines*, 6(2):28, 2018.

27. City of New York. COVID-19 data. Online, 2020 (accessed August 31, 2020). https://www1.nyc.gov/site/doh/covid/covid-19-data-testing.page.

28. Kristina L Bajema, Ryan E Wiegand, Kendra Cuffe, Sadhna V Patel, Ronaldo Iachan, Travis Lim, Adam Lee, Davia Moyse, Fiona P Havers, Lee Harding, et al. Estimated sars-cov-2 seroprevalence in the us as of september 2020. *JAMA Internal Medicine*, 2020.

29. Daniel B Larremore, Bailey K Fosdick, Kate M Bubar, Sam Zhang, Stephen M Kissler, C. Jessica E. Metcalf, Caroline Buckee, and Yonatan Grad. Estimating SARS-CoV-2 seroprevalence and epidemiological parameters with uncertainty from serological surveys. *medRxiv*, 2020.

30. Dennis Ellenberger, Ronald A Otten, Bin Li, Michael Aidoo, I Vanessa Rodriguez, Carlos A Sariol, Melween Martinez, Michael Monsour, Linda Wyatt, Michael G Hudgens, et al. HIV-1 DNA/MVA vaccination reduces the per exposure probability of infection during repeated mucosal SHIV challenges. *Virology*, 352(1):216–225, 2006.

31. Kate E Langwig, Andrew R Wargo, Darbi R Jones, Jessie R Viss, Barbara J Rutan, Nicholas A Egan, Pedro Sá-Guimarães, Min Sun Kim, Gael Kurath, M Gabriela M Gomes, et al. Vaccine effects on heterogeneity in susceptibility and implications for population health management. *mBio*, 8(6), 2017.

32. Paula Span. Older adults may be left out of some COVID-19 trials. *New York Times*, June 19, 2020. https://www.nytimes.com/2020/06/19/health/vaccine-trials-elderly.html.

33. Hannah R Sharpe, Ciaran Gilbride, Elizabeth Allen, Sandra Belij-Rammerstorfer, Cameron Bissett, Katie Ewer, and Teresa Lambe. The early landscape of coronavirus disease 2019 vaccine development in the UK and rest of the world. *Immunology*, 160:223 – 232, 2020.

34. Meryl Kornfield. When will children get a coronavirus vaccine? not in time for the new school year, experts fear. *Washington Post*, December 2, 2020. https://www.washingtonpost.com/health/2020/12/02/kids-vaccine-delay/.

35. Jennifer M Dan, Jose Mateus, Yu Kato, Kathryn M Hastie, Caterina Faliti, Sydney I Ramirez, April Frazier, D Yu Esther, Alba Grifoni, Stephen A Rawlings, et al. Immunological memory to sars-cov-2 assessed for greater than six months after infection. *bioRxiv*, 2020.

36. Christopher I Jarvis, Kevin Van Zandvoort, Amy Gimma, Kiesha Prem, CMMID COVID-19 working group, Petra Klepac, G James Rubin, and W John Edmunds. Quantifying the impact of physical distance measures on the transmission of COVID-19 in the UK. *BMC Med*, 18(124), 2020.

37. Jantien A Backer, Liesbeth Mollema, Don Klinkenberg, Fiona RM van der Klis, Hester E de Melker, Susan van den Hof, and Jacco Wallinga. The impact of physical distancing measures against covid-19 transmission on contacts and mixing patterns in the netherlands: repeated cross-sectional surveys. *medRxiv*, 2020. https://www.medrxiv.org/content/10.1101/2020.05.18.20101501v2.

38. Selene Ghisolfi, Ingvild Almas, Justin Sandefur, Tillmann von Carnap, Jesse Heitner, and Tessa Bold. Predicted COVID-19 fatality rates based on age, sex, comorbidities, and health system capacity. *Center for Global Development*, 2020.

39. Marc Lipsitch and Natalie E Dean. Understanding covid-19 vaccine efficacy. *Science*, 370(6518):763–765, 2020.

40. Lotty E Duijzer, Willem L van Jaarsveld, Jacco Wallinga, and Rommert Dekker. Dose-optimal vaccine allocation over multiple populations. *Production and Operations Management*, 27(1):143–159, 2018.

41. Takehiro Takahashi, Mallory K. Ellingson, Patrick Wong, Benjamin Israelow, Carolina Lucas, Jon Klein, Julio Silva, Tianyang Mao, Ji Eun Oh, Maria Tokuyama, Peiwen Lu, Arvind Venkataraman, Annsea Park, Feimei Liu, Amit Meir, Jonathan Sun, Eric Y. Wang, Arnau Casanovas-Massana, Anne L. Wyllie, Chantal B.F. Vogels, Rebecca Earnest, Sarah Lapidus, Isabel M. Ott, Adam J. Moore, Yale IMPACT research team, Albert Shaw, John B. Fournier, Camila D. Odio, Shelli Farhadian, Charles Dela Cruz, Nathan D. Grubaugh, Wade L. Schulz, Aaron M. Ring, Albert I. Ko, Saad B. Omer, and Akiko Iwasaki. Sex differences in immune responses that underlie COVID-19 disease outcomes. *Nature*, pages 1–6, 2020.

42. Dimple Chakravarty, Sujit S. Nair, Nada Hammouda, Parita Ratnani, Yasmine Gharib, Vinayak Wagaskar, Nihal Mohamed, Dara Lundon, Zachary Dovey, Natasha Kyprianou, and Ashutosh K.

Tewari. Sex differences in SARS-CoV-2 infection rates and the potential link to prostate cancer. *Communications Biology*, 3(374), 2020.

43. Monica Webb Hooper, Anna María Nápoles, and Eliseo J. Pérez-Stable. COVID-19 and Racial/Ethnic Disparities. *JAMA*, 323(24):2466–2467, June 2020.

44. Melissa Jenco. CDC vaccine committee may prioritize health care workers for COVID-19 vaccines. *AAP News*, August 2020. https://www.aappublications.org/news/2020/08/27/covid19vaccinepriorities082620.

45. Jon Cohen. The line is forming for a COVID-19 vaccine. Who should be at the front. *Science*, 369(6499):15–16, 2020.

46. Sharmistha Mishra, Jeffrey C. Kwong, Adrienne K. Chan, and Stefan D. Baral. Understanding heterogeneity to inform the public health response to COVID-19 in Canada. *CMAJ*, 192(25):E684–E685, 2020.

47. Laura Hawks, Steffie Woolhandler, and Danny McCormick. COVID-19 in Prisons and Jails in the United States. *JAMA Internal Medicine*, 180(8):1041–1042, August 2020.

48. Hamada S Badr, Hongru Du, Maximilian Marshall, Ensheng Dong, Marietta M Squire, and Lauren M Gardner. Association between mobility patterns and COVID-19 transmission in the USA: a mathematical modelling study. *The Lancet Infectious Diseases*, 2020.

49. Jamie Ducharme. These maps show how drastically COVID-19 risk varies by neighborhood. *Time*, 2020. https://time.com/5870041/COVID-19-neighborhood-risk/.

50. Kate M. Bubar, Kyle Reinholt, Stephen M. Kissler, Marc Lipsitch, Sarah Cobey, Yonatan H. Grad, and Daniel B. Larremore. COVID-19 vaccine prioritization code. Online, 2020. https://zenodo.org/badge/latestdoi/268932356.

51. R Core Team. *R: A Language and Environment for Statistical Computing*. R Foundation for Statistical Computing, Vienna, Austria, 2019.

52. Kendall E. Atkinson. *An Introduction to Numerical Analysis*, chapter 2, pages 56–58. Wiley, 2 edition, 1989.

53. WHO Global Health Observatory. Life tables by country. Online, 2016 (accessed December 3, 2020). https://apps.who.int/gho/data/view.main.LT62160?lang=en.

Acknowledgements: The authors wish to thank Sereina Herzog, Mark Jit, Jacco Wallinga, and Helen Johnson for their feedback. **Funding:** KMB was supported in part by the Interdisciplinary Quantitative Biology (IQ Biology) PhD program at the BioFrontiers Institute, University of Colorado Boulder. KMB and DBL were supported in part through the MIDAS Coordination Center (MIDASNI2020-2) by a grant from the National Institute of General Medical Science (3U24GM132013-02S2). ML, SMK, and YHG were supported in part by the Morris-Singer Fund for the Center for Communicable Disease Dynamics at the Harvard T.H. Chan School of Public Health. **Author Contributions:** KMB, SMK, ML, SC, YKG and DBL conceived of the study. KMB and DBL performed the analyses. KMB and KR generated all figures. KR created interactive visualization tools. All authors wrote and revised the manuscript. **Competing Interests:** ML discloses honoraria/consulting from Merck, Affinivax, Sanofi-Pasteur, and Antigen Discovery; research funding (institutional) from Pfizer, and an unpaid scientific advice to Janssen, Astra-Zeneca, and Covaxx (United Biomedical). **Data and materials availability:** Reproduction code is open source and provided by the authors (*50*).

included in the article that is credited to a third party; obtain authorization from the rights holder before using such material.

Supplementary Materials List:

Materials and Methods

Supplementary Text S1

Supplementary Figures S1 to S10

Supplementary Tables S1 and S2

Supplementary Materials For:

Model-informed COVID-19 vaccine prioritization strategies by age and serostatus

Kate M. Bubar,[1,2*] Kyle Reinholt,[3] Stephen M. Kissler,[4] Marc Lipsitch[4,5], Sarah Cobey[6], Yonatan H. Grad[4], Daniel B. Larremore[3,7*]

[1]Department of Applied Mathematics, University of Colorado Boulder, Boulder, CO, 80303, USA
[2]IQ Biology Program, University of Colorado Boulder, Boulder, CO, 80309, USA
[3]Department of Computer Science, University of Colorado Boulder, Boulder, CO, 80309, USA
[4]Department of Immunology and Infectious Diseases, Harvard T.H. Chan School of Public Health, Boston, MA, 02115, USA
[5]Center for Communicable Disease Dynamics, Harvard T.H. Chan School of Public Health, Boston, MA, 02115, USA
[6]Department of Ecology and Evolutionary Biology, University of Chicago, Chicago, United States
[7]BioFrontiers Institute, University of Colorado Boulder, Boulder, CO, 80303, USA

*To whom correspondence should be addressed;
E-mail: kate.bubar@colorado.edu and daniel.larremore@colorado.edu

This PDF file includes:

- Materials and Methods
- Supplementary Text S1
- Figs. S1 to S10
- Table S1 to S2

Materials and Methods

Susceptible Exposed Infectious Recovered (SEIR) Model Overview

We used a continuous-time system of ordinary differential equations (ODE) compartmental model stratified by age. All individuals were assumed to be initially susceptible, unless they had been effectively vaccinated or had naturally acquired immunity, which was considered to be protective in this model. Susceptible people (S) transition to the exposed state (E) after contact with an infectious individual. After a latent period, exposed individuals become infectious (I). After an infectious period, individuals move to a recovered state (R). We assume that recovered individuals are no longer infectious and are immune to reinfection. The duration of time spent in compartments E and I, in expectation, are specified in Table S1. Model equations were solved using *lsoda* ODE solver from the package 'deSolve', R version 3.6.0 (*51*). Fig. S1 shows model schematic diagrams for the variations of the SEIR model considered in this manuscript.

The force of infection, λ_i for a susceptible individual in age group i is

$$\lambda_i = u_i \sum_j c_{ij} \frac{I_j + I_{vj} + I_{xj}}{N_j - D_j},$$

where u_i is the probability of a successful transmission given contact with an infectious individual, c_{ij} is the number of age-j individuals that an age-i individual contacts per day, and $(I_j + I_{vj} + I_{xj})/(N_j - D_j)$ is the probability that a random age-j individual is infectious. To calculate the basic reproductive number, R_0, we define the next-generation matrix as

$$M = D_u C D_{d_I},$$

where D_u is a diagonal matrix with diagonal entries u_i, C is the country-specific contact matrix, and D_{d_I} is a diagonal matrix with diagonal entries d_I, where d_I is the infectious period. R_0 is the absolute value of the dominant eigenvalue of M. Age-stratified susceptibility values were drawn from literature estimates (*13*).

Incorporation of Vaccination, Vaccine Rollout, and Vaccine Efficacy

In the simplest version of the model, the vaccine is assumed to be transmission- and infection- blocking, and to work with variable efficacy. We considered two classes of scenarios. In the first class of scenarios, vaccinations are given in advance of model dynamics, which we call anticipatory vaccination. In the second class of scenarios, vaccinations are rolled out at the same time as the model dynamics, which we call continuous rollout vaccination.

In anticipatory vaccination scenarios, all the available vaccines were distributed at the initial time step, prior to the epidemic. To incorporate vaccinations, we initialized the model by dividing the total population of each age group between the susceptible compartment (S) and vaccinated compartment (V), according to the vaccine prioritization strategy and number of vaccines available. In anticipatory vaccination scenarios, the model was seeded with one infected person in each age group. Scenario 3 of the Main Text uses anticipatory rollout.

In continous rollout scenarios, vaccine rollout was parameterized by the percentage of the total population that could be vaccinated in each day of simulation, with values ranging from 0.25% to 2% of total population (see Fig. S3). Scenarios 1 and 2 of the Main Text consider rollout speeds of 1% per day. The prescribed number of individuals were vaccinated in simulations prior to the start of each day, such that disease dynamics proceeded in continuous time while vaccine rollout was computed in discrete steps. In continuous rollout scenarios, the model was seeded with 0.5% of individuals in each age group infected.

We considered two ways to implement vaccine efficacy (ve): as an all-or-nothing vaccine, where the vaccine provides perfect protection to a fraction ve of individuals who receive it, or as a leaky vaccine, where all vaccinated individuals have reduced probability ve of infection after vaccination (See Supplementary Text S1). We ran simulations with both types of vaccine efficacy, with figures in the Main Text showing results only for all-or-nothing vaccines.

To incorporate an age-dependent vaccine efficacy (see Fig. 3), we parameterized the relationship between age and vaccine efficacy via an age-efficacy curve with (i) a baseline efficacy, an age at which

efficacy begins to decrease (hinge age), and a minimum vaccine efficacy ve_m for adults 80+. We assumed that ve is equal to the baseline value for all ages younger than the hinge age, then decreases stepwise in equal increments for each decade to the specified minimum ve_m for the 80+ age group. To determine whether there exists a ve_m such that the mortality-minimizing strategy switches from directly vaccinating adults 60+ to an alternative strategy, we used the bisection method (*52*).

Incorporation of Existing Seroprevalence

To incorporate existing seroprevalence and compare areas with differing naturally-acquired immunity, we used data and seroprevalence estimates from Connecticut [low seroprevalence; (*28*)] and New York City [moderate seroprevalence; (*27*)]. To model high seroprevalence, we simulated an unmitigated epidemic until 40% seroprevalence was reached. Seroprevalence was implemented by moving the proportion of seropositive individuals from each age group into the recovered compartment, R, prior to forward simulations.

The model's implementation of vaccination depended on whether the vaccine was rolled out during ongoing transmission or prior to transmission, i.e. as an initial condition. For anticipatory vaccination without consideration of serostatus, v_i doses are given to the population, a fraction θ_i of whom are already seropositive. Thus, the total number of individuals eligible for vaccination are $S + R$, assuming people in I do not seek vaccination. The initial conditions are listed in Table S2, where $sp = 1, se = 0$. In dose redirection scenarios where vaccination is targeted only at seronegative individuals, simulations were conducted with sensitivity 96.7% and specificity 97.5%. Details of continuous vaccine rollout with dose redirection using an imperfect serological test can be found in Supplementary Text S1.

Calibration to achieve target R_0

Models were calibrated to achieve the target R_0 by multiplying the next-generation matrix by a constant to achieve the desired dominant eigenvalue, i.e. R_0. Because the constant factors out of the next-generation matrix equation, this may be mathematically interpreted as scaling up or down either the

contact rates C or susceptibilities u. All model calibration was performed prior to the inclusion of age-stratified seroprevalence or vaccination, meaning that the reproductive number R in the first days of a simulation may differ from R_0 depending on the scenario considered. Values of R_0 studied ranged from 1.3 to 2.6.

Measurement of outcomes: infections, deaths, and years of life lost

We ran simulations for 365 days to focus on the early prioritization phase of the COVID-19 vaccination programs. To compare the impact of different vaccination prioritization strategies, we calculated the cumulative number of infections and deaths. Infected individuals either move to the recovered or dead compartment, according to the age-dependent IFR (*19*) (see Fig. S1). The total number of estimated deaths was the number of people in the dead compartment at the end of the simulation. To calculate years of life lost from a death at a particular age (YLL), we multiplied standard life expectancy (SLE) by the number of deaths per age bin. We used the country-specific SLE estimates from the WHO Global Health Observatory (*53*), aggregated into age bins by decade using $YLL_i = \frac{1}{10}\sum_j YLL_j$ where j are the ages corresponding to decadal age bin i.

Contact Matrices and Demographics

Country-specific contact matrices include four types of contact: home, work, school, and other (*21*). In all simulations, we used total contact matrices, equivalent to the sums of the four contact types. Age demographics in all simulations were taken from the UN World Population Prospects 2019 (*22*) for each country. Age bins in each case were originally provided in 5-year increments, which were then combined into 10-year increments by addition. For instance, the number of individuals between 20 and 29 was the sum of individuals 20-24 and 25-29. The number of individuals 80 years and older was calculated as the sum of all age bins greater than 80.

We made two adaptations to existing contact matrices (*21*). First, we combined their five year age bins into ten year bins. Each entry in the matrices from Ref. (*21*) x_{ij} corresponds to the number of

individuals of age-group j that a person in age group i typically comes into contact with. Thus, for a country with population fraction d_i in age group i, the combined contact matrix entries are given by

$$c_{ij} = \frac{d_{2i}(x_{2i,2j} + x_{2i,2j+1}) + d_{2i+1}(x_{2i+1,2j} + x_{2i+1,2j+1})}{d_{2i} + d_{2i+1}} .$$

Second, we extrapolated matrices to include individuals 80+. To extrapolate, we copied the contact rates from 70-79 y.o. to our new row and column for 80+, along the diagonal. Then we filled in the end of our new row and column with the 70-79 y.o. contact rates with 0-9 y.o., assuming interactions with 0-9 y.o. are similar for people 70+. Lastly, to account for increased housing in long term living facilities for 80+ y.o., we decreased their contacts for 0-60 y.o. by 10% and added it to the 70 and 80 y.o. contacts. Thus, 80+ year-olds have the same total number of contacts as 70-79 year-olds, but relatively fewer among 0-69-year-olds and proportionally more among 70+ year-olds.

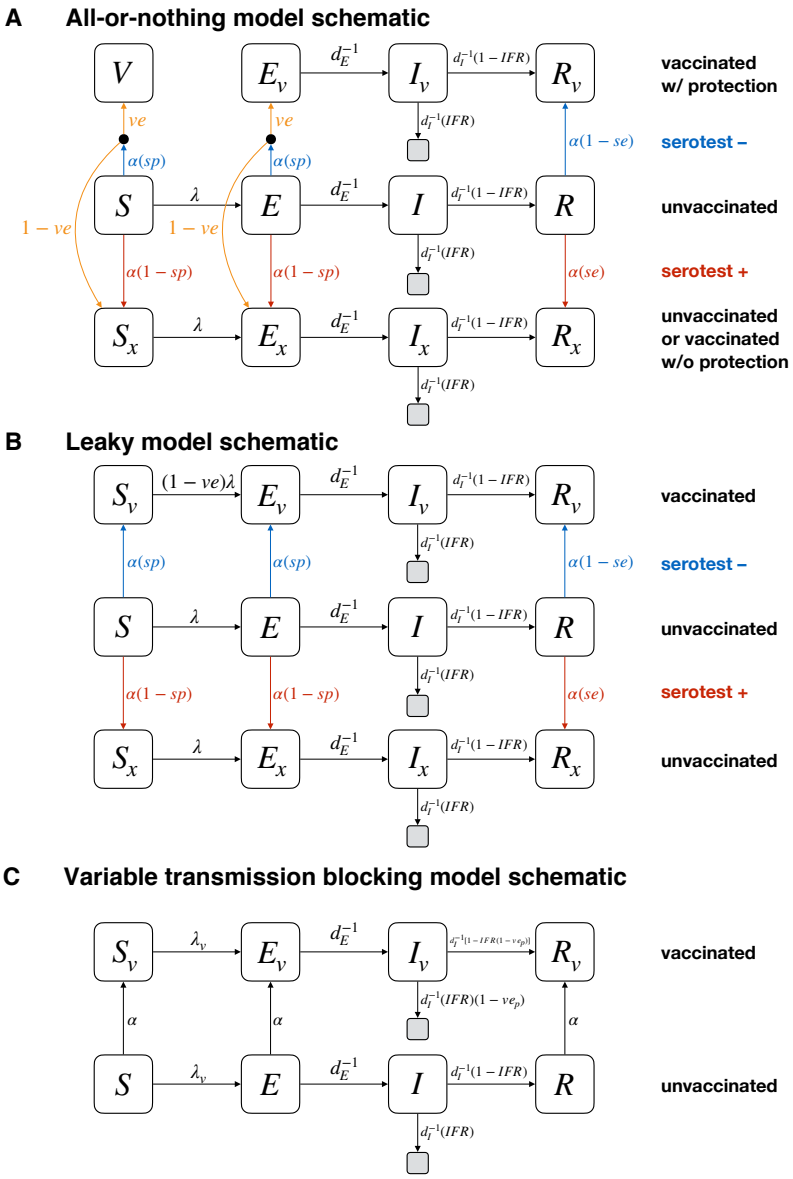

Figure S1: **Schematics for vaccine modeling framework.** Diagrams show compartmental models and transition rates for the (A) all-or-nothing, (B) leaky, and (C) variable transmission-blocking vaccine models used in this manuscript. S, E, I, and R represent susceptible, exposed, infectious, and recovered compartments; V represents a perfectly protected and vaccinated compartment; subscripts of v and x denote those who have been vaccinated with protection (v), and those who have either not been vaccinated or have been vaccinated but without protection (x). Grey unlabeled compartments represent death. The incorporation of a point-of-care serological test can be included by using known sensitivity se and specificity sp, or can be excluded by setting $se = 0$ and $sp = 1$ (a convenient mathematical representation of the no-test scenario as a test that always returns a negative result). Test rollout rate α is given by $\alpha = n_{\text{vax}}/\left[(S + E)sp + R(1 - se)\right]$. All compartments are stratified by age, in the text, with index i. See text for details and initial conditions.

Supplementary Text

S1 SEIR Model Modifications

The flexible age-stratified SEIR model framework allowed us to model (i) leaky or all-or-nothing vaccine efficacy, (ii) variable rollout speeds, (iii) point-of-care reprioritization of vaccines using an imperfect serological test, and (iv) the possibility of only partial transmission blocking effects, through straightforward modifications. The framework is shown in Fig. S1, and explicitly tracks individuals who were vaccinated and protected, vaccinated but not protected (all-or-nothing model only), considered for vaccination but did not receive a dose due to a positive serological test, and those who were not vaccinated or considered for vaccination. These four modes of operation are described in the subsections below.

S1.1 Implementing vaccine efficacy: leaky vs all-or-nothing

A vaccine with imperfect efficacy can be modeled as either a "leaky" vaccine, where all vaccinated individuals are ve protected against infection (Fig. S1A), or an "all-or-nothing" vaccine, where a fraction ve of vaccinated individuals are perfectly protected while the remaining (1- ve) individuals gain no protection (Fig. S1B). We considered both model implementations of vaccine efficacy, showing results for the all-or-nothing model in the Main Text and the leaky model in Supplementary Figures, as indicated in figure captions.

S1.2 Implementing variable vaccine rollout rate

We allowed vaccines to be distributed (or "rolled out") at different rates by parameterizing the number of vaccines available in each simulated day n_{vax}. In each simulated day, exactly n_{vax} doses are distributed, according to the prioritization strategy, prior to calculating new exposures, infections, and recoveries. As a result, anticipatory vaccination, in which all doses are used prior to SEIR dynamics, can be implemented by setting n_{vax} equal to the total number of doses available. In all scenarios, when all doses have been used, $n_{\text{vax}} = 0$ for all timesteps thereafter.

S1.3 Implementing point-of-care dose redirection with imperfect serological tests

The modeling framework depicted in Fig. S1 allows for the point-of-care reprioritization of tests by using the outcome of an imperfect serological test with sensitivity se and specificity sp. We assume that only those who test negative receive a vaccine, but that this population may consist of true negatives from the S or E compartments or false negatives from the R compartment. By tracking all such individuals, we prevent the model from vaccinating the same person twice. Similarly, we assume that those who test positive do not receive a vaccine at any point after testing positive. These include false positives from the S and E compartments and true positives from the R compartment.

The numbers of individuals who receive a vaccination each timestep, given a supply of n_{vax} to be allocated in that timestep, are

$$\begin{aligned} S \to S_v &= \frac{n_{\text{vax}}}{(S+E)sp + R(1-se)} S(sp) \\ E \to E_v &= \frac{n_{\text{vax}}}{(S+E)sp + R(1-se)} E(sp) \\ R \to R_v &= \frac{n_{\text{vax}}}{(S+E)sp + R(1-se)} R(1-se) \end{aligned} \tag{S1}$$

while the numbers of individuals who are tested but are excluded from vaccination are

$$\begin{aligned} S \to S_x &= \frac{n_{\text{vax}}}{(S+E)sp + R(1-se)} S(1-sp) \\ E \to E_x &= \frac{n_{\text{vax}}}{(S+E)sp + R(1-se)} E(1-sp) \\ R \to R_x &= \frac{n_{\text{vax}}}{(S+E)sp + R(1-se)} R(se) \end{aligned} \tag{S2}$$

How many more susceptible individuals get vaccinated when point-of-care reprioritization in used? This can be computed *a priori* for anticipatory rollouts in which a fraction θ_i of individuals in subpopulation i are truly seropositive and thus treated as recovered. If we further assume no ongoing transmission, then $S = (1-\theta_i)N$, and the number of susceptible individuals vaccinated is

$$\frac{n_{\text{vax},i}}{(1-\theta_i)sp + \theta_i(1-se)} (1-\theta_i)sp \,,$$

while the number of susceptible individuals vaccinated without point-of-care serology ($se = 0$, $sp = 1$) is

$$n_{\text{vax},i}(1 - \theta_i) \ .$$

The relative increase in the number of individuals vaccinated (one minus the ratio of these two counts) is thus

$$\text{relative increase in susceptibles vaccinated} = \frac{sp}{(1-\theta_i)sp + \theta_i(1-se)} - 1 \ , \tag{S3}$$

suggesting that a test with 96.7% sensitivity and 97.5% specificity in a population with 25% true seropositives would lead to a 32% increase in susceptibles vaccinated. When vaccine rollout is not anticipatory, and instead continues alongside transmission, *a priori* calculations of this type are not possible.

S1.4 Implementing vaccines with imperfect transmission blocking

We considered a vaccine that prevents severe manifestations of COVID-19 infection, including death, but imperfectly blocks transmission of SARS-CoV-2 (Fig. S1C). To model such a vaccine, we modify the leaky vaccine model by introducing three different mechanisms for vaccine efficacy: ve_S is the efficacy of the vaccine to decrease susceptibility; ve_I is the efficacy of the vaccine to decrease infectiousness; and ve_P is the efficacy of the vaccine to decrease the likelihood that the infection progresses to severe disease and death.

In this model, the infectiousness of vaccinated individuals is decreased by a factor of $1-ve_I$. Second, the susceptibility of vaccinated individuals is decrease by a factor of $1 - ve_S$. This results in a force of infection for unvaccinated individuals of

$$\lambda_i = u_i \sum_j c_{ij} \frac{(I_j + (1 - ve_I)I_j^V)}{N_j - D_j}$$

and a force of infection for vaccinated individuals of

$$\lambda_{i,V} = (1 - ve_S)\lambda_i \ .$$

These values of λ_i replace previous values of λ_i for $S \to I$ transitions, and values of $\lambda_{i,V}$ replace values of $(1-ve)\lambda_i$ for $S_V \to I_V$ transitions (see Fig. S1). Finally, the fatality rate, conditioned on infection, is multiplied by a factor of $1 - ve_P$.

The impact of this non-transmission blocking model on minimizing incidence and mortality are shown in Supplementary Fig. S7 for $ve_S = 0$, $ve_P = 90\%$ and $ve_I = 0 - 100\%$. Note that when $ve_S = ve_I = 0$, there are no indirect effects of vaccination. Finally, we note that when considering a leaky vaccine with different effects on infection, transmission, and progression, the parameterization could be accomplished in any of several ways. Ours makes the choice for simplicity to consider the vaccine's entire effect to be on infectiousness and progression.

Supplementary Figures

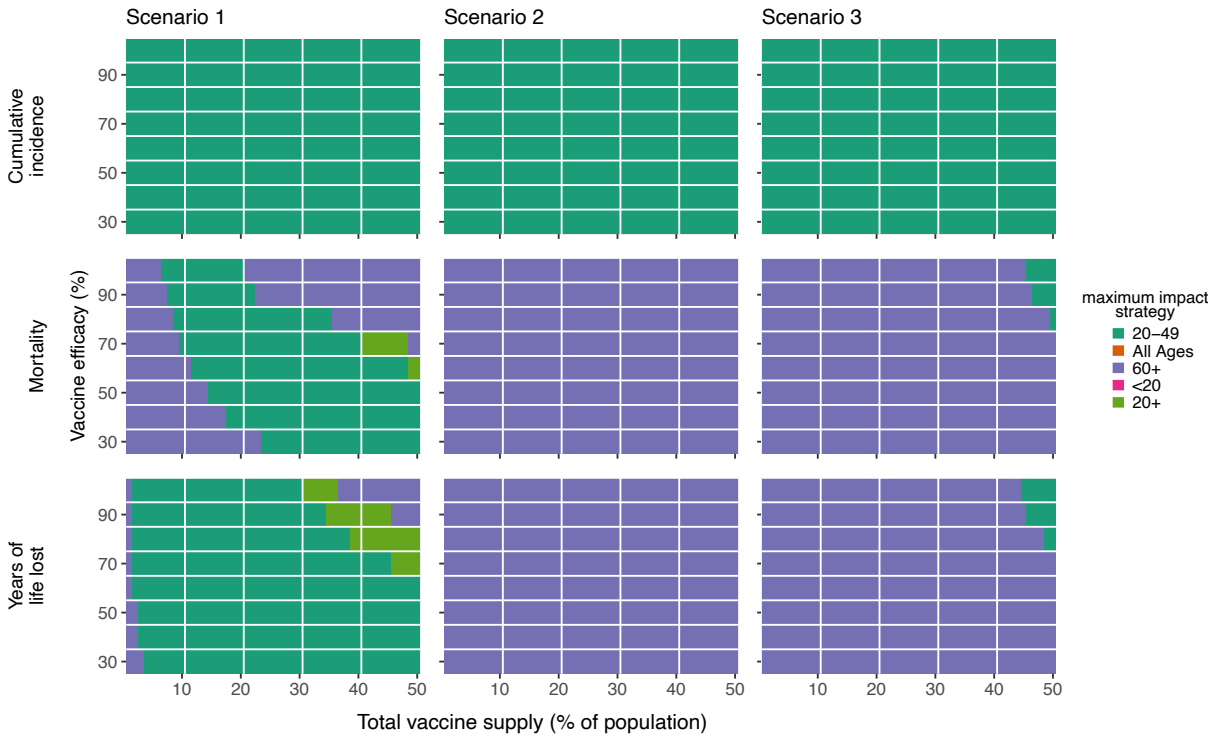

Figure S2: **Impact of vaccine efficacy on maximum impact strategies (all-or-nothing vaccine).** Heatmaps show the prioritization strategies resulting in maximum reduction of infections (top row), mortality (middle row), and years of life lost (bottom row) across Scenario 1 (1% rollout/day, $R_0 = 1.3$; left column), Scenario 2 (1% rollout/day, $R_0 = 2.6$; middle column), and Scenario 3 (anticipatory rollout, $R_0 = 2.6$; right column). Each heatmap shows results from simulations varying vaccine supply and vaccine efficacy as indicated. Shown: contact patterns and demographics of the United States (*21, 22*); all-or nothing and transmission blocking vaccine. See Fig. S4 for leaky vaccine results.

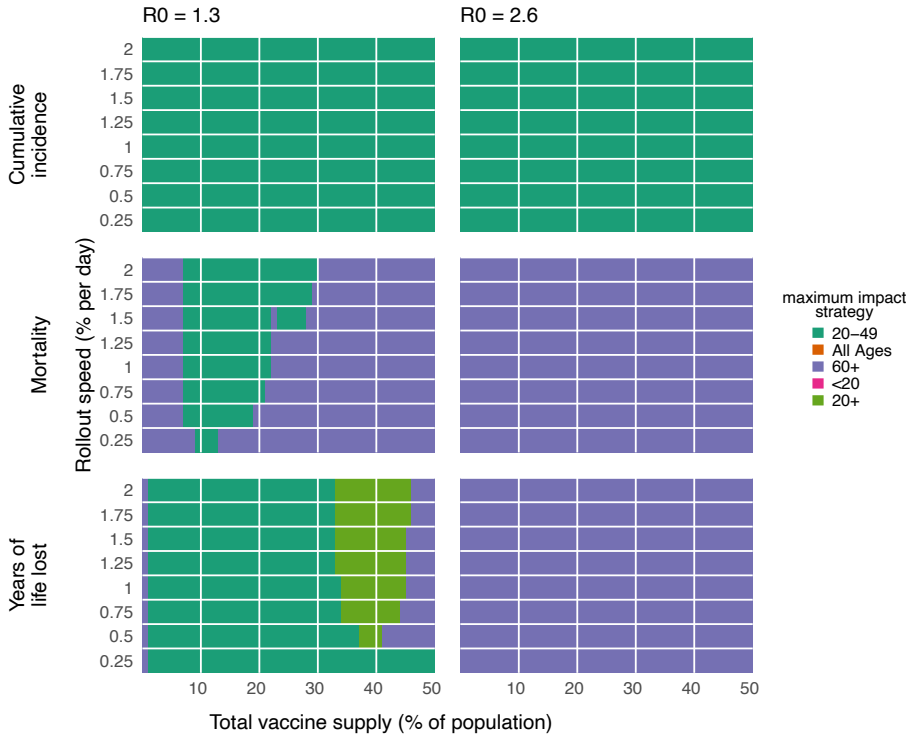

Figure S3: **Impact of rollout speed on maximum impact strategies.** Heatmaps show the prioritization strategies resulting in maximum reduction of infections (top row), mortality (middle row), and years of life lost (bottom row) for $R_0 = 1.3$ (left column) or $R_0 = 2.6$ (right column). Each heatmap shows results from simulations varying vaccine supply and the rollout speed of the vaccine, measured in the percentage of the total population vaccinated per day. Shown: contact patterns and demographics of the United States (*21, 22*); all-or nothing and transmission blocking vaccine, $ve = 90\%$.

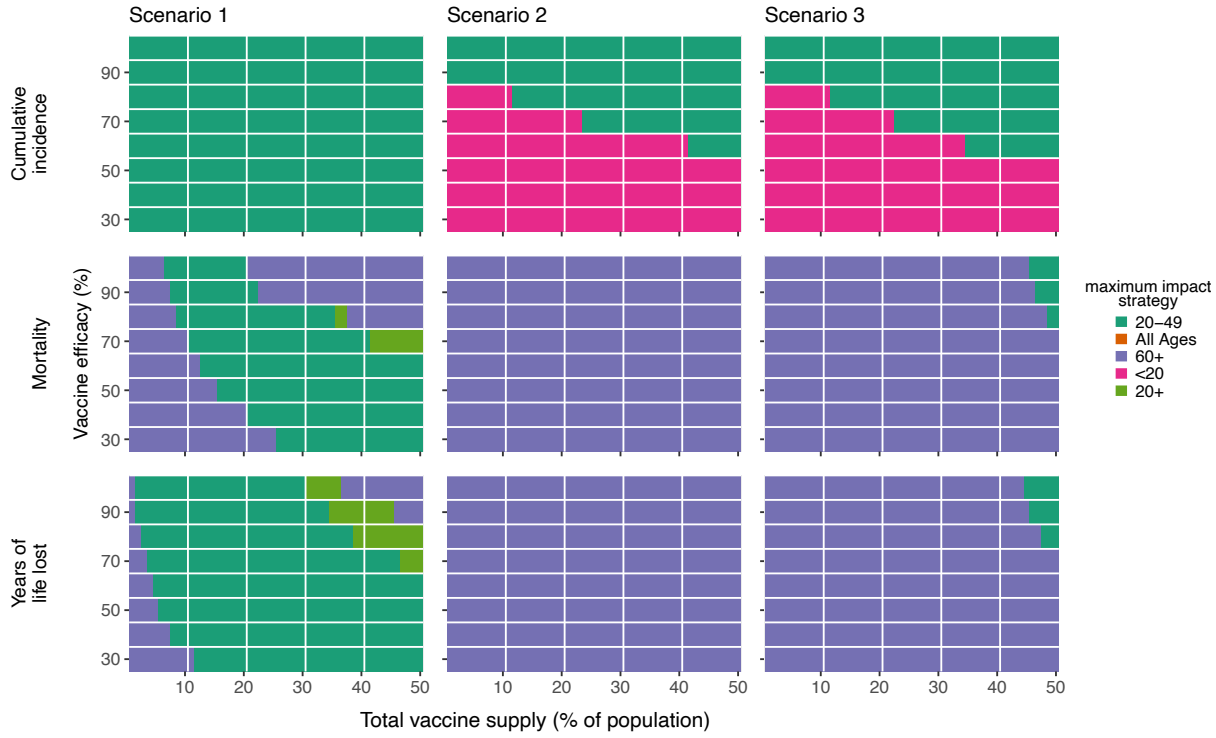

Figure S4: **Impact of vaccine efficacy on maximum impact strategies (leaky vaccine).** Heatmaps show the prioritization strategies resulting in maximum reduction of infections (top row), mortality (middle row), and years of life lost (bottom row) across Scenario 1 (1% rollout/day, $R_0 = 1.3$; left column), Scenario 2 (1% rollout/day, $R_0 = 2.6$; middle column), and Scenario 3 (anticipatory rollout, $R_0 = 2.6$; right column). Each heatmap shows results from simulations varying vaccine supply and vaccine efficacy as indicated. Shown: contact patterns and demographics of the United States (*21, 22*); leaky and transmission blocking vaccine. See Fig. S2 for all-or-nothing vaccine results.

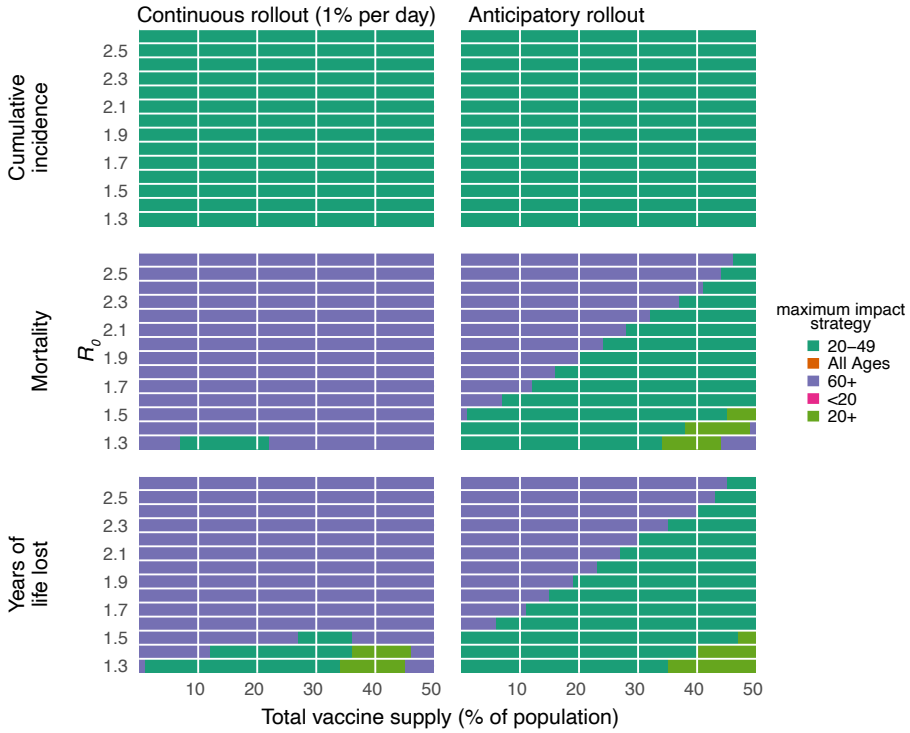

Figure S5: **Impact of reproductive number $\mathbf{R_0}$ on maximum impact strategies.** Heatmaps show the prioritization strategies resulting in maximum reduction of infections (top row), mortality (middle row), and years of life lost (bottom row) for a continuous rollout scenario (1% rollout/day; left column) or an anticipatory rollout scenario (all doses administered prior to simulations; right column). Each heatmap shows results from simulations varying vaccine supply and the basic reproductive number transmission R_0. Shown: contact patterns and demographics of the United States (*21, 22*); all-or nothing and transmission blocking vaccine, $ve = 90\%$.

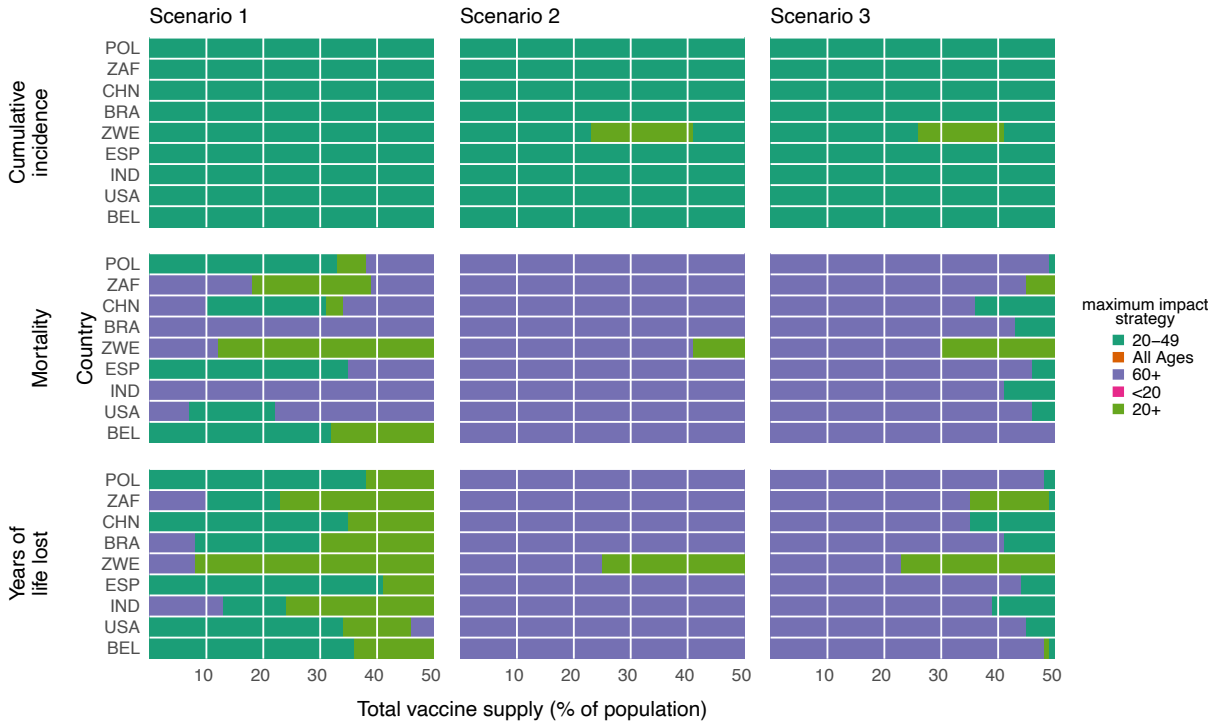

Figure S6: **Impact of country demography and contact patterns on maximum impact strategies.** Heatmaps show the prioritization strategies resulting in maximum reduction of infections (top row), mortality (middle row), and years of life lost (bottom row) across Scenario 1 (1% rollout/day, $R_0 = 1.3$; left column), Scenario 2 (1% rollout/day, $R_0 = 2.6$; middle column), and Scenario 3 (anticipatory rollout, $R_0 = 2.6$; right column). Each heatmap shows results from simulations varying vaccine supply and the country whose demographics and contact patterns were modeled (*21, 22*). Shown: all-or-nothing and transmission blocking vaccine, $ve = 90\%$. POL, Poland; ZAF, South Africa; CHN, China; BRA, Brazil; ZWE, Zimbabwe; ESP, Spain; IND, India; USA, United States of America; BEL, Belgium

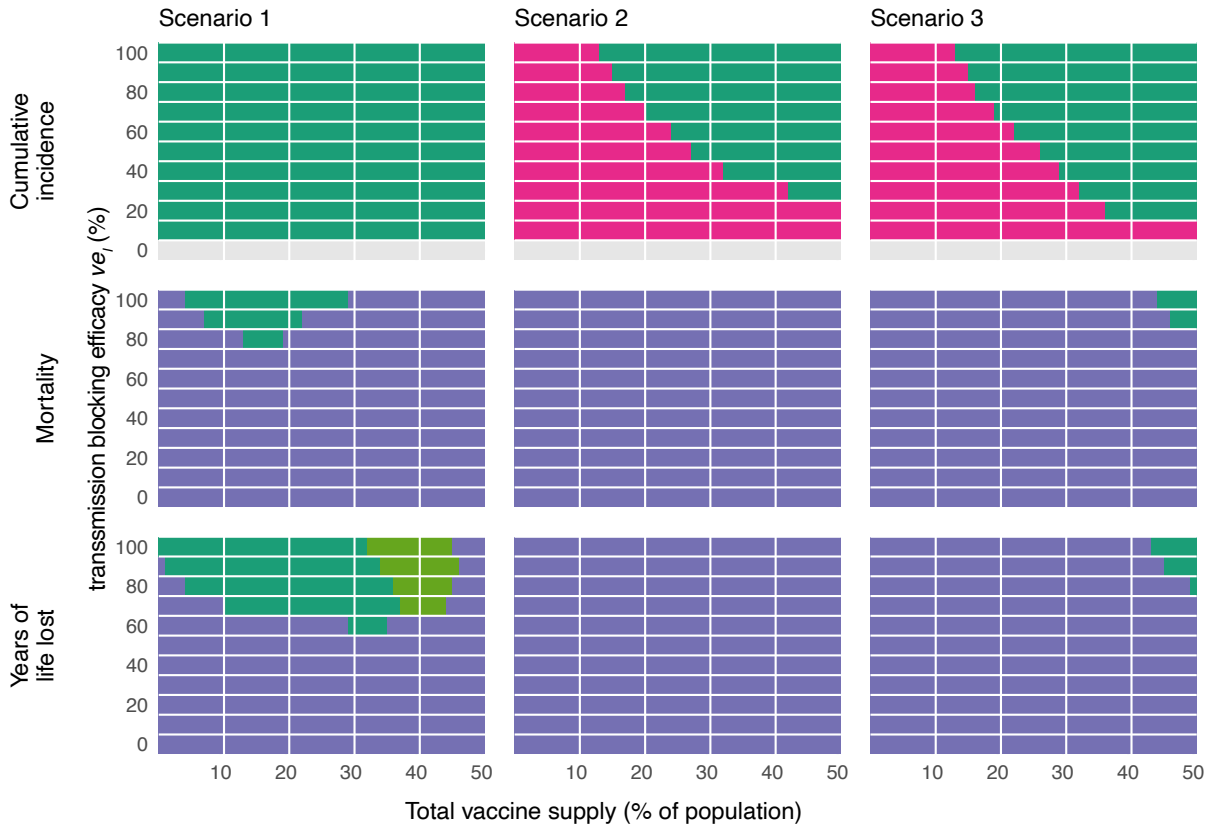

Figure S7: **Impact of imperfect transmission-blocking effects on maximum impact strategies.** Heatmaps show the prioritization strategies resulting in maximum reduction of infections (top row), mortality (middle row), and years of life lost (bottom row) across Scenario 1 (1% rollout/day, $R_0 = 1.3$; left column), Scenario 2 (1% rollout/day, $R_0 = 2.6$; middle column), and Scenario 3 (anticipatory rollout, $R_0 = 2.6$; right column). Each heatmap shows results from simulations varying vaccine supply and the vaccine's efficacy in blocking transmission ve_I as indicated. Shown: contact patterns and demographics of the United States (*21, 22*), for a vaccine with protective efficacy from severe disease $ve_P = 0.9$ and no efficacy for protection from infection $ve_S = 0$. See Supplementary Text S1 for modeling details.

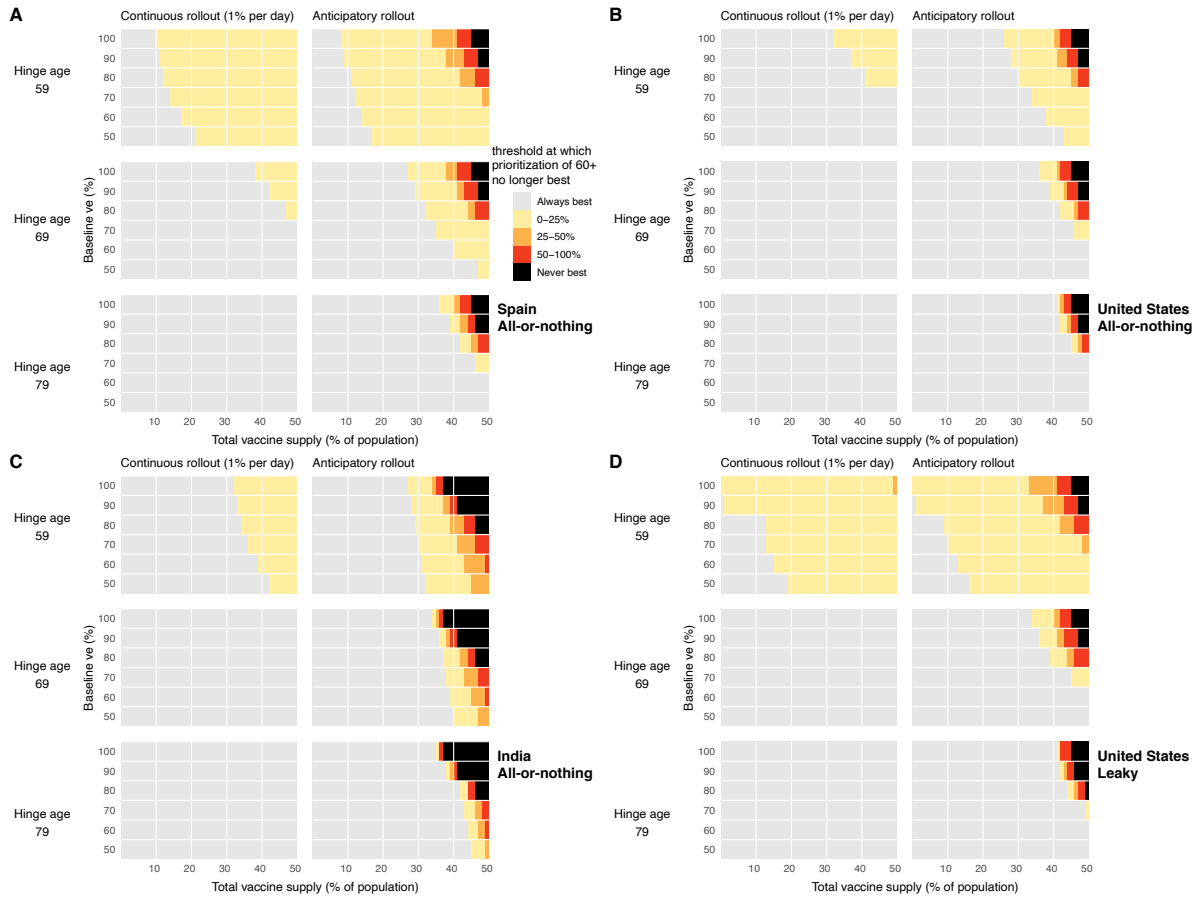

Figure S8: **Impact of age-related decreases in vaccine efficacy on vaccine prioritization.** Heatmaps show that prioritization of adults 60+ to minimize mortality remains generally robust to large decreases in vaccine efficacy among older adults. Each point shows the threshold value of vaccine efficacy among adults 80+ at which prioritizing adults 60+ is no longer the best strategy to minimize mortality, if one exists (yellow, orange, red), or indicates that none exists (grey). Parameter combinations for which mortality is never minimized by prioritization of adults 60+ are also shown (black). Panels show combinations of the age at which immunosenescence begins (hinge age), total vaccine supply, and baseline efficacy for continuous and anticipatory rollout scenarios ($R_0 = 2.6$) for (A) Spain, (B) the United States, and (C) India, using an all-or-nothing vaccine model; (D) the United States, using a leaky vaccine model.

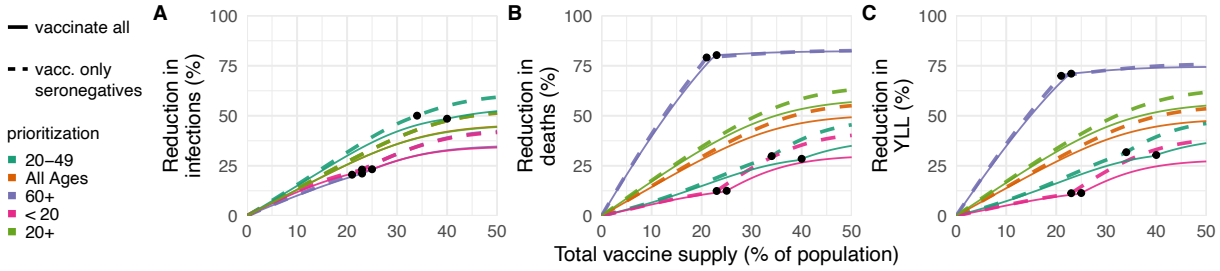

Figure S9: **Effects of existing seropositivity on the impacts of prioritization strategies (low seroprevalence).** Percent reductions in (A) infections, (B) deaths, and (C) years of life lost (YLL) for prioritization strategies when existing age-stratified seroprevalence is incorporated (July 2020 estimates for Connecticut; mean seroprevalence 3.4% (*28*)). Plots show reductions for Scenario 2 (1% rollout/day, $R_0 = 2.6$, realized $R = 2.55$) when vaccines are given to all individuals (solid lines) or to only seronegatives (dashed lines), inclusive of imperfect serotest sensitivity and specificity. Shown: contact patterns and demographics for the United States (*21, 22*); all-or-nothing and transmission-blocking vaccine with $ve = 90\%$. See Figs. 4 and S10 for moderate and higher seroprevalence examples, respectively.

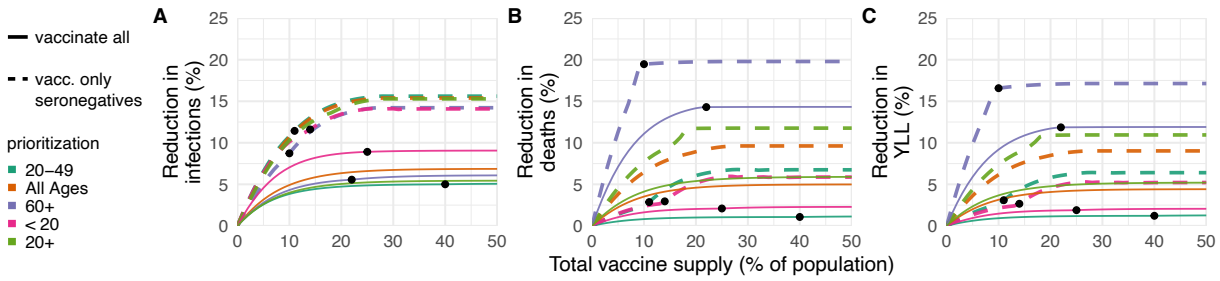

Figure S10: **Effects of existing seropositivity on the impacts of prioritization strategies (high seroprevalence).** Percent reductions in (A) infections, (B) deaths, and (C) years of life lost (YLL) for prioritization strategies when existing age-stratified seroprevalence is incorporated (model-generated; mean seroprevalence 39.5%; see Methods) and intial conditions are set to the S, E, I, and R compartment counts at the mid-outbreak time when seroprevalence reached 39.5%. Plots show reductions for Scenario 2 (1% rollout/day, $R_0 = 2.6$, realized $R = 1.45$) when vaccines are given to all individuals (solid lines) or to only seronegatives (dashed lines), inclusive of imperfect serotest sensitivity and specificity. Shown: U.S. contact patterns and demographics (*21, 22*); all-or-nothing and transmission-blocking vaccine with $ve = 90\%$. See Figs. 4 and S9 for moderate and lower seroprevalence examples, respectively.

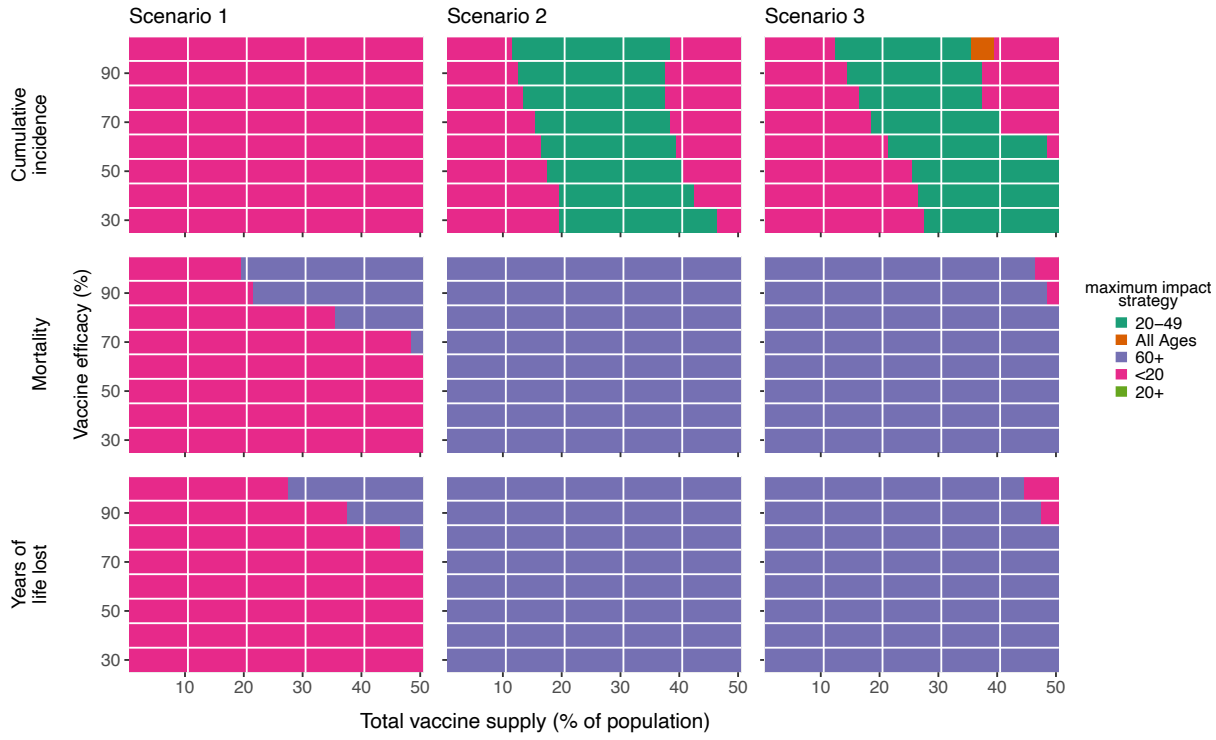

Figure S11: **Impact of vaccine efficacy on maximum impact strategies (all-or-nothing vaccine; constant susceptibility by age).** Heatmaps show the prioritization strategies resulting in maximum reduction of infections (top row), mortality (middle row), and years of life lost (bottom row) across Scenario 1 (1% rollout/day, $R_0 = 1.3$; left column), Scenario 2 (1% rollout/day, $R_0 = 2.6$; middle column), and Scenario 3 (anticipatory rollout, $R_0 = 2.6$; right column). Each heatmap shows results from simulations varying vaccine supply and vaccine efficacy as indicated, but unlike all other simulations in this manuscript and its supplementary material, except Fig. S12, simulations use a constant susceptibility by age Shown: contact patterns and demographics of the United States (*21, 22*); all-or nothing and transmission blocking vaccine. See Fig. S12 for leaky vaccine results with constant susceptibility by age. See Fig. S2 for all-or-nothing vaccine results with varying susceptibility by age.

Figure S12: **Impact of vaccine efficacy on maximum impact strategies (leaky vaccine; constant susceptibility by age).** Heatmaps show the prioritization strategies resulting in maximum reduction of infections (top row), mortality (middle row), and years of life lost (bottom row) across Scenario 1 (1% rollout/day, $R_0 = 1.3$; left column), Scenario 2 (1% rollout/day, $R_0 = 2.6$; middle column), and Scenario 3 (anticipatory rollout, $R_0 = 2.6$; right column). Each heatmap shows results from simulations varying vaccine supply and vaccine efficacy as indicated, but unlike all other simulations in this manuscript and its supplementary material, except Fig. S11, simulations use a constant susceptibility by age. Shown: contact patterns and demographics of the United States (*21, 22*); leaky and transmission blocking vaccine. See Fig. S11 for all-or-nothing vaccine results with constant susceptibility by age. See Fig. S4 for leaky vaccine results with varying susceptibility by age.

Supplementary Tables

Parameter	Description	Value	Reference
d_E	Latent period	3 days	(*13*)
d_I	Infectious period	5 days	(*13*)
u_i	Relative susceptibility to infection for age-i individuals*	[0.4, 0.38, 0.79, 0.86, 0.8, 0.82, 0.88, 0.74, 0.74]	(*13*)
IFR	Infection fatality rate	[0.001, 0.003, 0.01, 0.04, 0.12, 0.40, 1.36, 4.55, 15.24]	(*19*)
N_i	Number of people in age group i	country-specific demographic data	(*22*)
θ_i	Percent of seropositive age-i individuals	New York**: [32.0, 31.29, 24.9, 24.9, 26.4, 27.9, 25.75, 22.15, 20.7] Connecticut**: [3.9, 3.82, 3.1, 3.1, 3.1, 3.7, 3.2, 2.7, 2.7]	(*15, 27*)
c_{ij}	Number of age-j individuals contacted by an age-i individual per day	Country-specific contact matrix (home, work, school and other)	(*21*)

Table S1: **Summary of parameters used in modeling and simulation.**
* Relative susceptibility shown here is scaled in practice to give R_0 of interest.
** To relate NYC (*27*) and US (July/August, 2020; Connecticut chosen because it was the median of overall seroprevalence estimates reported in Bajema et al (*28*)) seroprevalence estimates to age bins by decade, we computed
$\theta_i = (\sum_j \theta_j)/10$ where j is the ages in bin i.

IC*	**Anticipatory rollout, all-or-nothing** ve	**Anticipatory rollout, leaky** ve	**Continuous rollout**
$I_i(0)$	1		0.005 N_i
$R_i(0)$	$\theta_i N_i - \alpha_i \theta_i N_i$		$\theta_i N_i$
$R_{Vi}(0)$	$\alpha_i \theta_i N_i (1 - se)$		0
$R_{Xi}(0)$	$\alpha_i \theta_i N_i se$		0
$S_i(0)$	$[N_i - I_i(0) - \theta_i N_i] - \alpha_i [N_i - I_i(0) - \theta_i N_i]$		$N_i - I_i(0) - \theta_i N_i$
$S_{Vi}(0)$	NA	$\alpha_i [N_i - I_i(0) - \theta_i N_i](sp)$	0 if leaky ve, else NA
$V_i(0)$	$\alpha_i [N_i - I_i(0) - \theta_i N_i] ve(sp)$	NA	0 if all-or-nothing ve, else NA
$S_{Xi}(0)$	$\alpha_i [N_i - I_i(0) - \theta_i N_i](1 - sp) -$ $\alpha_i [N_i - I_i(0) - \theta_i N_i](1 - ve)(sp)$	$\alpha_i [N_i - I_i(0) - \theta_i N_i](1 - sp)$	0

Table S2: **Initial conditions for simulations.** Scenario initial conditions (ICs) are reported for scenarios considered in this manuscript. Vaccination rollout $\alpha = n_{\text{vax}} / [(S + E)sp + R(1 - se)]$. Situations with no dose redirection via serological testing are equivalent to setting $sp = 1$ and $se = 0$.
* ICs for all other compartments not explcitily specified are 0.